Application of artificial neural network for prediction of fluoride removal efficiency using neutralized activated red mud from aqueous medium in a continuous fixed bed column.

Anil Kumar Giri (anilchemnit@gmail.com)
Fakir Mohan University https://orcid.org/0000-0001-9723-1881
Prakash Chandra Mishra
Fakir Mohan University

Research Article

Keywords: Neutralized activated red mud, Fluoride, Artificial neural network, Continuous fixed bed, Bed height, Character-ization

Posted Date: June 21st, 2022

DOI: https://doi.org/10.21203/rs.3.rs-1702568/v1

Abstract

The present research work approaches the removal of fluoride from aqueous medium using neutralized activated red mud (NARM) in a continuous fixed bed column. Artificial neural network (ANN) technique was applied effectively for optimization of the model for the practicability of the removal process. The consequences of various experimental variables like bed length, adsorbate concentration, experimental time and adsorbate solution flow rate studied to know the breakthrough point and saturation times. The highest removal potentiality of NARM was considered to be 3.815 mg g^{-1} of F^- in the bed height of 15 cm, starting concentration 1ppm, susceptible time 120 minutes, adsorbate solution flow rate 0.5 $mLmin^{-1}$, and constant room temperature, respectively. Bohart-Adams and Thomas models were considered to describe the fixed bed column effect to the bed height and adsorbate concentrations. The experimental data were applied a back propagation (BP) learning algorithm programme with four-seven-one architecture model. The artificial neural network model was considered to be functioning correctly as absolute relative percentage error, which is 0.671 throughout the learning period. Differentiation between the predicted out comes from ANN model and actual results from experimental analysis affords a high degree of correlation (R^2 = 0.998) stipulating that the model was able to predict the adsorption efficiency. Experimented adsorbent materials was characterized using different instrumental analysis that is SEM-EDS, FTIR and XRD.

Introduction

Population detonation, anomalous climate condition, development of modern civilization, metropolitan city development, rapidly progress industries, and advanced technology has been generated enormous amounts of toxicants to the severe contamination both in ground and surface water bodies (Wang et al. 2018; **Chakraborty and Das 202)**. The water pollution arises due to the different environmental condition that brings consequential consideration of its remediation skills and techniques (Mukherjee and Halder 2018; Nguyen et al. 2013). Current situation in India fluoride infected in ground water has been ascertained more than 20 state and 66 million people are distress from fluorosis disease. As a result of higher concentration and longtime contamination of fluoride ions reveals a lot of problems formed on the human health. Accordingly, the World Health Organization (WHO) has suggested the standard concentration of 1.5 mgL^{-1} F^- in drinking water purposes **(**Wan et al. 2021; Ali et al. 2016). This limit has recommended a challenge for present research of new technologies capable of selectively removing low level of F^-. In contemplation of fluoride analysis in water, developed a cost-efficient innovation to bring out fluoride from aqueous medium a great consciousness at the end of 20 year (Mohapatra et al. 2009; Khandare and Mukherjee 2019; Deshmukh et al. 2009; Sivasankar et al. 2010; Daifullah et al. 2007). Traditionally various conventional and non-conventional techniques have been enforced to eliminated F^- from contaminated water bodies. Adsorbent surface assimilation technique is an adsorption process of best application of adsorbate ions completely separated out from aqueous medium. It is a very simple technique, economically very less, cost-efficient and environmentally friendly nature (Camargo 2003; Gandhi et al. 2012; Chen et al. 2021; Angelin et al. 2021; **Alagumuthu and Ranjan 2010a**). Red mud is an eccentric waste material and possessions of different high amounts of toxic heavy metals that is SiO_2 (3–50%), Al_2O_3 (10–20%), Fe_2O_3 (30–60%), CaO (2–8%), Na_2O (2–10%), TiO_2 (trace-10%) as well as assemblage of minor ingredients likely K, Cr, V, Ni, Ba, Cu, Mn, Pb, and Zn (Sahu et al. 2010). Consequently, development and carry out its storage, remediation programs remain essential, and its inventory grows approximately 120 million per annum. The red mud can be simply transported from the dumping site to the nearby residential areas. Contact of the red mud cause serious threat to the ground water by seepage and also causes various environmental hazards **(**Tor et al. 2009; He et al. 2013; Bhatnagar et al. 2011). Neutralized activated red mud prepared from fresh red mud, and its use for the fixed bed column adsorption of the F^- from aqueous medium has not been reported. The highest F^- removal efficiency using fixed bed column from aqueous medium of different activated adsorbents are presented in Table 1. Adsorption treatment process is a complicated method because of different parameters are interconnection with the removal process. Artificial neural network (ANN) is a powerful prediction tool for the identification of the relevant parameters and their correlation relationships are very complex. Removal of toxicants from aqueous solutions using different prediction models has been used current time by numbers of researchers (Chen et al. 2021; Wan et al. 2021). The main objectives of the current research works were using a multilayer feed forward neural network model to forecast the removal of F^- from aqueous medium using fixed bed column study. The input paraments encompass adsorbate concentration,

fixed bed height, experimental time, and adsorbate flow rate whereas removal of F^- is considered as output results. The prophesy of breakthrough curve point is calculated from different fixed bed column length and adsorbate concentration using Bohart-Adams and Thomas equation. The total experimental results can be separated into learning and inference set, if the network system is well trained, the ANN model can be tested with any data to optimization the best outcome. To know the adhesion of F^- exterior sit of the NARM using different instrumental characterization that is SEM-EDS, FTIR and XRD.

Materials And Methods

Preparation of adsorbent and reagents

The collected fresh red mud samples were first grinded in motor pestle and the powder was sieved by 450 mm sieving machine. Then, 20 gm of fresh red mud powder was taken a 250 ml washed container and added 100 ml deionized water to it and mixed properly. The counterbalance form of fresh red mud by slowly put in 1N HNO_3 and 1N NaOH fresh prepared solutions. The assert of pH all experimental analysis was operating a calibrated pH Systronics pH meter-335. After added required amounts of 0.1N HNO_3 and 0.1N NaOH to be form neutralized activated red mud and it's dried at 110 º C for 24 hours in oven. Afterwards, 50 gm neutralized red mud was taken in a 250 ml washed dry container and added slowly 70 ml (98% mm^{-1}) of sulphuric acid, then after 10 minutes reaction 30 ml of concentrated nitric acid (65% mm^{-1}) was added in to the sample. Consequently, the treated samples were kept 24 hours in well maintained oven, after that the prepared samples were washed four times carefully using deionized water further put in oven at 120 100 ºC for completely dried. Figure 1 manifest a graphically encapsulated detailed preparation procedure of activated neutralized red mud from fresh red mud. The physico-chemical parameters of the neutralized activated red mud results are particle size (100–240 µm), pH (7), moisture contained (8.01%), conductivity (21.13 µS cm^{-1}), specific gravity (0.31), porosity (81%), bulk density (0.55 gmL^{-1}), ion-exchange capacity (0.79 $meqg^{-1}$), water soluble matter 1.16%), volatile matter (41%), respectively. The specific surface area of neutralized activated red mud is found to be 212.02 m^2g^{-1} (Brunauer-Emmett-Teller surface area analyzer, Quantachrome AUTOSORB-1, USA). All experimental analysis, standard preparation and chemical reagent preparation using fresh collected deionized water. 1000 ppm of fluoride stock solutions was processed by adding 0.221 gram of NaF solutions in a 1 liter of deionized water, this stock solutions having 10 ppm of F^-. Subsequently, to prepared a sequence of standard fluoride solution, desirably 0.5ppm F^- by dilution of the stock solutions (Greenberg et al. 2005; Miretzky and Cirelli 2011).

Fixed bed column studies

Fluoride removal from contaminated water in a fixed bed column experiments by neutralized activated red muds were carried out using standard 0.1ppm, 1ppm, 5ppm and 10ppm fluoride solution in the absence of other competing ions. Column studies were accomplished in a glass column of 6 cm internal diameter, 50 cm bed height, and samples flow rate are asserted by a burette, respectively (Fig. 1). In the bottom portion of the glass column was placed a purified cotton to the prevent any loss of sample materials and mechanical support to the filtrate bed. Total experiment was carried out at room temperature. Effects of process parameters like fixed bed column height (adsorbent dosage) was assorted as 5 cm (6.50 gram), 10 cm (12 gram) and 15cm (18.5 gram), fluoride concentration is assorted as 1ppm, 5ppm, and 10ppm, experimented duration was assorted as 10 min – 150 min and flow rate of sample was assorted as 0.5 $mLmin^{-1}$, 2,5$mLmin^{-1}$ and 5.5 mL min^{-1} were investigated. Experimented samples were collected desired time period from the bottom of the glass column and tested to know the F^- concentration in the samples. After treated each sample was allowed to settle 10 min and it's centrifuged at 1000 rpm for 20 min and filtered through Whatmann 42µ size filter paper. The concentrations of the F^- before and after adsorption were determined by Orion star A214 Fluoride electrode (Thermo Scientific). The continuous fixed bed column potentiality was evaluated by the breakthrough time period and removal quantity given in Eq. 1(Chen et al. 2021; Tor et al. 2009). To know the effective efforts of the fixed bed glass column systems applying various easy numerical models were succeeded. In the present research work has been approach two simple mathematical models that is Bohart-Adams and Thomas. Bohart-Adams model indicated that the rate of the removal process is corresponding to the part of removal efficiency persist on the sorbent materials. Bohart-Adams model can be intimated in equations 2 &3 (Chen et al. 2021; Ye et al. 2018; Sivasankar et al. 2010).

Thomas model is supposition rate driving forces comply pseudo-second-order kinetics reversible reaction (Chawdhury and Saha 2013; Hiremath and Theodore 2017; Tor et al. 2009; Mohan et al. 2017). This model can be described in Eq. 4.

Column breakthrough equation (q_B) = $\left(\frac{x}{m}\right)_B = \frac{x_B}{m_{adsorbent}} = Q_v \left(C_0 - \frac{C_B}{2}\right) \frac{t_B}{m_{adsorbent}}$ (1)

Bohart-Adams equation $ln\left(\frac{C_t}{C_0}\right) = K_{AB} C_o t - K_{AB} N_0 \left(\frac{Z}{U}\right)$ (2)

Maximum removal efficiency (q_o) = $\frac{NoZS}{X}$ (3)

Thomas equation = $\frac{C_t}{C_0} = \frac{1}{1+\exp\left(\left(K\frac{th}{F}\right)\left(q_{0X-C_0V_{ef}}\right)\right)}$ (4)

Where C_0 is the initial adsorbate concentration in ppm, C_t is the removal of adsorbate ions in ppm with respect to experimental time period in minutes, x_B is the mass of adsorbate ions removed in the fixed bed column at breakthrough (mg), m is the mass of the NARM in the column (g), Qv is the flow rate ($mLmin^{-1}$), C_B is the breakthrough adsorbate ions concentration (mgg^{-1}), t_B is the experimental time to breakthrough (min), K_{AB} illustrated the Adams-Bohart kinetic constant (mgL^{-1}), N_0 is the saturation concentration(mgL^{-1}), t is the sample flow time (min), Z stands for fixed bed column depth (cm), and U is the linear flow rate ($mLmin^{-1}$), S stands for bed cross section area (cm^2) and X stand for unit mass of adsorbent packed in the glass column (g). K_{th} is the Thomas rate constant ($mLmg^{-1}min^{-1}$), q_0 is the maximum capacity of adsorption (mgg^{-1}), X quantity of the adsorbent in the column (g). V_{ef} is volume of solution (mL) and F is the flow rate ($mLmin^{-1}$).

Back propagation neural network model (BPNN)

The adsorbate ions removal effectiveness calculated using different analytical appliances are intricated because-of complication of the system. So, the artificial neural network system is embraced to enhance the forecast ability of removal efficiency at contact time period. Accordingly, in the present research results implemented in ANN modelling for optimization purposes as a consequence of high potentiality of distinguished the input variables and output results in the convoluted condition. The back propagation neural network (BPNN) system comprising of three distinct layers. The first input layer (*P)* collects data from experimental analysis then proceeds this data into the network system for process of treating. The second hidden layer (*I*) obtained data from the input layer, after that all the collected data treating in the network system. Finally output layer (*Y*) accepts clarified data from the network system, then it conveys the outcomes to an outside effector. The shape of the back propagation network system manifested in Fig. 2. The neural network functioning system consists of two stages that is first learning or training stage and second inference or testing stage. The arrangement of this network system as it may be conferred E - I -Y, the input layer (*E*) stipulated by the number of input parameters. The input indicators are reform along associated with significance is known as performance factor (*Pmn*), which illustrates the connected of n^{th} neuron of the input layer to m^{th} neuron of the hidden layer. Similarly, the output indicators of hidden layer are reform by connected with performance factor (*Pom*) of O^{th} neuron of output layer to m^{th} node of the hidden layer. All the reform instruction used a logistic sigmoid transfer factor (*f*) are incorporated at the output layer (Liu et al. 2018; Nikzad et al. 2015; Wang et al. 2016).

Let $I_s = (I_{S1}, I_{S2}, I_{S3}\ldots\ldots\ldots I_{Si})$, S = 1,2,3……. *E* is S^{th} design among *E* input manner. Where *Pom and Pmn* are the relationship importance between n^{th} input neuron to m^{th} hidden neuron, and m^{th} hidden neuron to O^{th} output neuron, respectively. The estimated output results from a neuron in the input, hidden, and output layer using a mathematical equation described as:

$O_{sn} = E_{sn}$ e = 1,2…….. *E* (Input layer) (5)

$O_{sm} = f(\sum_{i=0}^{E} P_{mi} O_{si})$, m = 1,2,3..... *I* (Hidden layer) (6)

$O_{so} = f\left(\sum_{m=0}^{I} P_{om} O_{sm}\right)$, *o* = 1,2,3 ... *Y* (Output layer) (7)

All experimental analysis results are accomplished by MATLAB 7 using a Pentium IV PC mathematical software with the ANN toolbox (Saha et al. 2010). In present studies, the four input parameters (adsorbate solutions, fixed bed column height, experimental time, and adsorbate flow rate) are utilize in an artificial neural network software for desired output efficiency of the adsorbent by column studies. Presently 170 data are produced from laboratory analysis and it's separated into two sets that is learning and inference used for the modeling system. ANN network processing system seventy five percent data are used for the training set and twenty five percent data are used for testing set. All the data are conciliated in the 0.1–0.9 range to elude the measuring consequences of parameter values. By utilizing the actual and predicted conclusion to investigates the precision of artificial network system **(**Yetilmezsoy and Demirel 2008; Wang et al. 2018; Chawdhury and Saha 2013**)**. The finest evidence efforts of artificial network model achieve by utilizing the root mean square error (RMSE) described as:

$$\text{RMSE} = \sqrt{\frac{1}{n-p}\sum_{i=1}^{n}\left(q_{emodel} - q_{eexperimental}\right)^2} \quad (8)$$

where, $q_{e\ model}$ is the predicted result and $q_{e\ experimental}$ is the actual value for the i^{th} manner.

Results And Discussion

Consequences of fixed bed column length with experimental time on the breakthrough curve

The bed length is the key variable for the removal efficacious of fluoride from aqueous medium in the continuous fixed column studies. The breakthrough curve is illustrated the ratio between commencing concentration of fluorides /remaining concentration of fluoride in the experimental container (C_t/C_0) against the adsorbate solution flow rate time (t). **Fig. 3** described as the continuous fixed bed column removal process of fluoride at different bed heights 5 cm (**Fig. 3a**), 10 cm **(Fig. 3b**) and 15 cm (**Fig. 3c**), experimental time (10 - 150 minutes), at constant starting concentration 1 ppm, flow rate 0.5ml min^{-1}, room temperature, and at neutral pH, respectively. **Table 2** illustrated the mathematical results of fixed bed column with different bed height and experimental time of fluoride solutions. The bed height is strongly influenced the fixed bed column breakthrough saturation time and the adsorbent bed length performance. Mathematical results of breakthrough curve and saturation times increases with increase in length of bed height and exposed time of fluoride solution because of developed more numbers of attaching sites on the upper surface of the adsorbent during the removal processes **(Saha et al. 2010, Yetilmezsoy and Demirel 2008).** In the present studies shows that the breakthrough time increased with the increases in bed length. The maximum removal of fluoride is considered to be 3.815 mgg^{-1}, bed height 15cm, fluoride concentration 1ppm, flow rate 0.5 ml min^{-1}, at room temperature, respectively. When pH of the aqueous medium remains in a neutral range (pH=7) the fluoride removal onto the neutral adsorbent surface can be decreased by a ligand or ion exchange reaction mechanisms **(Chen et al. 2021, Ranasinghe et al. 2022, Ghorai and Pant 2005**). **Figure 3** manifested a differentiation between the ANN model predictions and the experimental data as a function of length of bed height. From this figure clearly shows that the ANN model satisfactorily predicts the trend of the experimental data.

Consequences of adsorbate concentration with experimental time on the breakthrough curve

Adsorbate concentrations is the major variable for the influence the removal effectiveness of fluoride ions in the continuous fixed bed column system. **Figure 4** delineation the continuous fixed bed column removal process of fluoride ions at different fluoride concentrations 1 ppm (**Fig.4a**), 5 ppm (**Fig. 4b**), and 10 ppm (**Fig. 4c**), experimental time (10-150 min), a constant length of bed height 15cm, flow rate 0.5 mL/min, neutral pH, and room temperature, respectively**.** At the maximum removal of fluoride ions shown in 1ppm because of on the surface of neutralized activated red mud bed saturated quickly leading to breakthrough and exhaust in time. The higher concentration of fluoride ions needs to disseminates on the exterior surface of

the adsorbents by intraparticle dissemination processes. So, the adsorbate to form hydrolysed ions will spread out slowly **(Chawdhury and Saha 2013).** Experimental results showed that the removal process reached equilibrium in about 120 min of flow rate for all concentrations of fluoride ions in this study. However, for initial fluoride ions concentrations of 1, 5 and 10 ppm, adsorption equilibrium percentages are determined to be higher than the fluoride concentration of 5 ppm. Hence, 1 ppm of fluoride ions concentration was selected as the optimal starting concentration for further breakthrough experiments. **Figure 4** represented the experimental results with comparison of ANN output results for different starting concentrations.

Consequences of adsorbate solutions flow rate with experimental time on the breakthrough curve

Flow rate is one of the most significant characteristics in evaluating the removal capability of the adsorbent for continuous fixed bed column treatment of fluoride containing aqueous solutions. The consequence of flow rate in the fixed bed column system with neutralized activated red mud is examined changing flow rate to 0.5 mL/min (**Fig. 5a**), 2.5 mL/min (**Fig. 5b**) and 5.5 mL/min (**Fig. 5c**) with constant fluoride concentration 1 ppm, neutral pH 7, bed height 15 cm, and room temperature, respectively. The highest removal of fluoride ions from aqueous medium shown in flow rate of 0.5 ml min^{-1} because of the residence time of the adsorbate was more at lower flow rate and so the adsorbent got more time for binding with fluoride ions effectively. For the higher flow rate 2.5 $mlmin^{-1}$ and 5.5ml min^{-1} the breakthrough curve (C_t/C_0) of fluoride are establish to increase at the initial part of the treatment but at the mean time flow rate time is increased in the operation time shows that decrease in removal ability. The speed of the initial concentration of the fluoride ions remarkably affected the contact between the surface of the adsorbate and adsorbent (**Chawdhury and Saha 2013, Joshi et al. 2020, Deshmukh et al. 2009**). The experimental data and ANN calculated outputs for various flow rate values are shown in **Fig. 5**.

Breakthrough curve analysis by Bohart-Adams and Thomas model

Bohart-Adams and Thomas models are appliance to forecast the continuous fixed bed column achievement variables. The consequences of breakthrough curves prognosticated analysis by the Bohart-Adams model are differentiated among the investigational result with different bed length and constant starting concentration of fluoride 10 ppm and outcomes are conferred in **Fig. 6a.** This model prognosticated the different variables observed from experimental data function as enhanced the fixed bed column performance. **Table 3** illustrated the various parameters results of this model are interpenetrate adsorbate concentration (N_0), Bohart-Adams rate constant (K_{AB}), adsorbate solution flow rate, and fluoride concentration, correlation coefficient, and root mean square error, respectively (**Chen et al. 2021, Chawdhury and Saha 2013)**. It is considerably from **Fig. 6a** and **Table 3** exhibits an impecunious concurrence between actual result and prognosticated results. In the current investigation, the interpenetrate adsorbate concentration (N_0) results gradually diminished among the enlargement of fixed bed length because of greater extent area are void for removal of fluoride ions. Concluded that the removal process is bestowal by the corporeal mass convey of the breakthrough curve analysis (**Geleta et al. 2022, Ghorai and Pant 2005**). Rate constant (K_{AB}) of this model is raised among the enlargement in the bed length disclosed the kinetics constant is conquered by extraneous mass convey in the beginning portion of the fixed bed column system. To conclude that, Bohart-Adams model handled a clear, understandable and extensive perspectives for evaluating the removal of fluoride ions from aqueous medium. **Figure 6b** indicated the consequences of breakthrough curves prognosticated analysis by the Thomas model are compared with the actual results. Different variables are estimated using Thomas model equation that is rate constant (K_{TH}) of Thomas model, maximal solid-phase concentration (q_0), adsorbate solution flow rate, fluoride concentration, correlation coefficient, root mean square error and the values are exhibited in **Table 3.** The diagrammatic and enumeration values exhibit a satisfactory concurrence among actual and prognosticated consequence suggests the Thomas model (**Deshmukh et al.2009, Zare et al. 2022**). In the present study, Thomas rate constant (K_{TH}) results reveals optimum at the moment concentration of fluoride is minimal denoted the fixed bed column removal process of the adsorbents is kinetically agreeable at minimal ranges of contamination. The solid phase concentration (q_0) is reduced among the rise in the fixed bed length as a consequence of the rate limiting step is moved from peripheral to inside mass convey. To concluded that, Thomas model presumed adsorption arise at particular uniform area inside of the materials and Pseudo-second order kinetics activities is suitable for breakthrough curve analysis (**Mohan et al. 2017, Sahu et al. 2020a**)

Prediction approach for removal efficiency using ANN model

The prophesy of removal efficacious of fluoride ions from water utilize activated neutralized red mud (ANRM) is a complicated hypothesis, consequently neural network prediction system approach is espoused. Total 168 investigational results assembled from laboratory observations after that separated into two sets that is 75 % (126) data are applied learning phase and 25 % (42) data are applied inference phase. Back propagation neural network probabilistic program along three layered based architectonic structure narrated aside arched convey assignment at input layer, one hidden layer is operated, and straightaway convey function is manipulated in an output layer, respectively and it's presented in **Fig. 2 (Rojas et al 2015**). Primarily, the learning results are furnished in to the neural network systems and its dissemination of output results (**Fig. 7).** The number of neurons used in the hidden layer is manifested by the connection of two into whole root over of the number of variables used in the input system plus one. In the network system to observe the best number of neurons at the hidden layer by determining the mean squared error (MSE) (**Yetilmezsoy and Demirel 2008, Chawdhury and Sahu 2013**). In present study, four number of variables are selected in the input layer, six neurons are chosen in the hidden layer since MSE commences diminish, and finally predicted results represented in one output layer. Training and impetus variables are put down at range 0.25 and 0.20, respectively (**Wang et al. 2016, Joshi et al. 2020)**. In the learning phase initially responsibility as the input results is transmitted ahead across the network system to enumerated the output result of each unit. The estimation of error indication for each output unit in the neural network system bank on predicted output results contrast with desired results. Root mean square error (RSME) is 0.371 calculated from neural network system depended upon the number of exhaustive overtake the learning results. **Figure 8a** represented as correlation coefficient (R^2 = 0.998) for learning set result observed from actual and predicted removal percentage of fluoride ions. In the course of inference phase the dissemination of output results and an extremity of correlation coefficient (R^2 = 0.987) between actual and predicted removal percentage of fluoride ions is achieved as shown in **Fig. 8b.** The mean absolute relative percentage error is considered to be 0.671 for learning and 0.640 for inference data set generated from neural network processing system. Juxtaposition results of the actual and predicted for inference data sets are shown in **Table 4.** The application of artificial neural network model is a best attempt towards enhancing the prediction coherence of adsorbate ions from aqueous medium. Even so, the present research work is consciousness on patterning of fluoride ions removal from water using a new ecofriendly adsorbent media by continuous fixed bed column method **(Giri et al. 2011, Liu et al.2018).** In general, investigational learning point of view functioning in the best effort of artificial neural network application in designing of intricated wastewater analysis.

Instrumental description of neutralized activated red mud

SEM-EDS (ZEISS Geminis SEM 360 model, German**)** images are obtained at 50.00 K x magnification with corresponding energy dispersive spectrum of the activated neutralized red mud (ANRM) prior to and afterward fluoride ions adsorption at neutral pH and it's illustrated in **Fig. 9.** Fresh neutralized activated red mud without approach of fluoride analysis distinctly displays the surface consistency, architecture and different range of apertures (**Fig. 9a**). Afterward neutralized activated red mud treated with 1 ppm fluoride ions evidently changes in the upper surface. It is distinctly noticed that the upper surface of the treated adsorbents has been changed into a novel glossy bit and crystals are embedded in the surface (**Fig. 9b**). The corresponding EDS spectra of neutralized activated red mud control and treated with 1 ppm of fluoride ions is shown in **Fig. 9a and 9b**. The EDS images distinctly indicates the presence of different elements that is C, O, Al, Fe, Si and F. SEM-EDS results are further validated with the analysis of FTIR (**Geleta et al. 2022, Sahu et al. 2020a**).

FTIR (Perkin Elmer FT-IR, RX-I) studies are done in order to know the functional groups and structure of the neutralized activated red mud. **Figure 10** delineation the spectra of neutralized activated red mud prior to and afterward removal of fluoride ions exhibits number of absorption peaks. The spectra of prior to and afterward removal of fluoride ions is illustrated in **Fig. 10a** and **Fig. 10b**. In the present FTIR analysis discloses distinctly some absorption band shifted from higher to lower frequency may be stretching or bending vibration with different functional groups. Fluoride ions feasibly complication to the numbers of absorption peaks that is 3,305.99 cm^{-1} is moved to 3,251.98 cm^{-1} because of cemented with -OH groups, 1, 631.78 cm -1 has been moved to1,600.92 cm^{-1} because of connected with N-H and C=O stretching vibration, 1,481.33 cm^{-1} has been moved to 1,419.61 cm^{-1} as a consequence of connected with N-H groups, and 887.28 cm^{-1} moved to 883.40 cm^{-1} because of

corresponding to the O-C-O scissoring vibration of polysaccharide, respectively **(Angelin et al. 2021, Rojas et al. 2015, Ye et al. 2018,Chen et al. 2021, Gandhi et al. 2012, Sivasankar et al. 2010, Prabh and Meenakshi 2014)**. Finally, concluded that the transfer of the spectra from higher frequency to lower frequency probably ascribed to the interconnection of F^- among the hydroxyl, amide and amino groups afford on the exterior surface of the neutralized activated red mud. XRD (PHILLIPS X'PERT X-ray diffractometer (model PW 1710) image of the neutralized activated red mud control and treated with 1ppm fluoride solution is shown in **Fig. 11**. Fresh neutralized activated red mud generally composed of different elements like O, Si, Al, Fe and Ti are exhibited in EDS image (**Fig. 9a**). The XRD data of the treated materials contributed evidence of decreases in the peak intensity which shows that adsorption of fluoride ions comparison with control materials. So, it was concluded that part of fluoride ions is converted into HF, some part of the converted into AlF_3 and another some parts converted into FeF_2 at neutral pH and finally fluoride ions adhesion on the surface of the neutralized activated red mud (**Zare et al. 2022, Chen et al. 2021**).

Conclusion

The present research work demonstrates successfully removal of fluoride from water in a continuous fixed bed column technique using neutralized activated red mud. The artificial neural network mathematical tool is applied effectively for the prediction of fluoride from water using neutralized activated red mud. Prediction efficiency is observed using backpropagation algorithm in three layered based neural network model. For learning and inference data set apply in neural network processing system generated mean absolute relative percentage error is 0.671 and 0.640, respectively. High degree correlation coefficient (R^2 = 0.995) is the learning data set and convey 0.37 root means square error estimated from neural network system. Behaviour of breakthrough modelling and equilibrium times exhibits the optimum removal ability is considered to be 3.815 mgg^{-1} at adsorbate solution flow rate 0.5 $mlmin^{-1}$, fixed bed column height 15 cm, fluoride concentration 1ppm, and normal room temperature, respectively. The better prophesy of breakthrough curve analysis is assessed by Bohart-Adams and Thomas model. The treated samples are analyzed by SEM-EDS, FTIR and XRD techniques. FTIR spectra may be attributed to the interaction of fluoride ions with the amide, amino and hydroxyl groups present exterior surface of the neutralized activated red mud. XRD pattern manifested part of fluoride ions converted into HF, AlF_3, and FeF_2. So, neutralized activated red mud is the best choice adsorbent media for fluoride ions removal from aqueous medium. Artificial neural network is a statistical prediction tool with high-speed confluent conceivably among investigational result to minimize analytical endeavor.

Declarations

Ethics approval and consent to participate: Present research work has been Application of artificial neural network for prediction of fluoride removal efficiency using neutralized activated red mud from aqueous medium in a continuous fixed bed column. The communicated manuscript does not involve the use of any animal or human data or tissue. So “Not applicable” in this section.

Consent for publication: This manuscript does not contain data from any individual person. So “Not applicable” in this section.

Availability of data and materials: Not Applicable

Competing interests: The authors declare that they have no competing interests.

Funding: Not Applicable

Authors' contributions: Anil Kumar Giri*[1], Prakash Chandra Mishra[2] help for preparation of the manuscript. contribution on adsorbent preparation, experimental setup, experimental analysis as well as help for preparation of the manuscript. **Anil Kumar Giri** has contribution all instrumental characterization and analysis of material as well as manuscript writing, checking, preparation of all figures and tables. Finally, all Authors read and approved the final manuscript.

Acknowledgement

The authors are thankful to Prof. S. K. Tripathy, Vice-Chancellor, Fakir Mohan University, Balasore and Odisha Higher Education Programme for Excellence & Equity (OHEPEE) assisted by World Bank for providing financial assistance and necessary facilities help to accomplish the research work.

Authors' information (optional)

References

1. Alagumuthu G, Rajan M (2010a) Equilibrium and kinetics of adsorption of fluoride onto zirconium impregnated cashew nut shell carbon. Chem Eng J 158:451–457
2. Ali S, Thakur SK, Sarkar A, Shekhar S (2016) Worldwide contamination of water by fluoride. Environ Chem Lett 14(3):291–315
3. Angelin A, Kalpana M, Govindan K, Kavitha S (2021) Characterizations and fluoride adsorption performance of wattle humus biosorbent. Environ Sci Pollution Res PMID 34145546. doi:10.1007/s11356-021-14864-9
4. Bhatnagar A, Vilar VJP, Botelho CMS, Boaventura RAR (2011) A review of the use of red mud as adsorbent for the removal of toxic pollutants from water and wastewater. Environ Technol 32(3–4):231–249
5. Camargo AJ (2003) Fluoride toxicity to aquatic organisms: a review. Chemosphere 50:251–264
6. Chakraborty V, Das P (2022) Investigation on efficiency of synthesized lanthanum oxide–coated biochar and graphene oxide–coated biochar on removal of fluoride: batch and fixed bed continuous reactor performance modelling. Biomass Convers Biorefinery. doi: 10.1007/s13399-022-02661-4
7. Chawdhury S, Saha PD (2013) Artificial neural network (ANN) modeling of adsorption of methylene blue by NaOH modified rice husk in a fixed-bed column system. Environ Sci Pollut Res 20(2):1050–1058
8. Chen F, Lv F, Li H, Xu L, Wei J, He Y, Qian J, Gao P (2021) Evaluation of fluoride adsorption in solution by synthetic Al_2O_3/CeO2: a fixed-bed column study. Water Environ Res. doi:10.1002/wer.1601
9. Daifullah AA, Yakout SM, Elreefy SA (2007) Adsorption of fluoride in aqueous solutions using $KMnO_4$ modified activated carbon derived from steam pyrolysis of rice straw. J Hazard Mater 147:633–643
10. Deshmukh WS, Attar SJ, Waghmare MD (2009) Investigation on sorption of fluoride in water using rice husk as an adsorbent. Nat Environ Pollut Technol 8:217–223
11. Gandhi N, Sirisha D, Shekar KBC, Asthana S (2012) Removal of fluoride from water and wastewater by using low-cost adsorbents. Int J Chem Tech Res 4:1646–1653
12. Geleta WS, Alemayehu E, Lannartz B (2022) Fixed-Bed Adsorption: Comparisons of Virgin and Zirconium oxide-coated scoria for the removal of fluoride from water. Molecules 27:1–20
13. Ghorai S, Pant KK (2005) Equilibrium, kinetics and breakthrough studies for adsorption of fluoride on activated alumina. Sep Purif Technol 42:265–271
14. Greenberg AE, Trussell RR, Clesceri LS (2005) Standard Methods for the Examination of Water and Wastewater, 16th edn. APHA AWWA WPCF Washington
15. He ZL, Zhang GK, Xu W (2013) Enhanced adsorption of fluoride from aqueous solution using an iron-modified attapulgite adsorbent. Water Environ Res 85(2):167–174
16. Hiremath PG, Theodore T (2017) Biosorption of Fluoride from Synthetic and Ground Water Using Chlorella vulgaris Immobilized in Calcium Alginate Beads in an Up Flow Packed Bed Column. Periodica Polytech Chem Eng 61(3):188–199
17. Joshi S, Bajpai S, Jana S (2020) Application of ANN and RSM on fluoride removal using chemically activated D. Sissoo saw dust. Environ Sci Pollut Res 27(15):17717–17729
18. Khandare D, Mukherjee S (2019) A review of metal oxide nanomaterials for fluoride decontamination from water environment. Materialstoday: Proceedings 18(3):1146–1155

19. Liu ZW, Liang FN, Liu YZ (2018) Artificial neural network modeling of biosorption process using agricultural wastes in a rotating packed bed. Appl Therm Eng 140:95–101
20. Miretzky P, Cirelli AF (2011) Fluoride removal from water by chitosan derivatives and composites: A review. J Fluorine Chem 132(4):231–240
21. Mohan S, Singh DK, Kumar V, Hasan SH (2017) Effective removal of Fluoride ions by rGO/ZrO_2 nanocomposite from aqueous solution: fixed bed column adsorption modelling and its adsorption mechanism. J Fluor Chem 194:40–50
22. Mohapatra M, Ananda S, Mishra BK, Giles DE, Singh P (2009) Review of fluoride removal from drinking water. J Environ Manage 91(1):67–77
23. Mukherjee S, Halder G (2018) A review on the sorptive elimination of fluoride from contaminated wastewater. J Environ Chem Eng 6(1):1257–1270
24. Nguyen TAH, Ngo HH, Guo WS, Zhang J, Liang S, Yue QY, Li Q, Nguyen TV (2013) Applicability of agricultural waste and by-products for adsorptive removal of heavy metals from wastewater. Bioresour Technol 148:574–585
25. Nikzad M, Movagharnejad K, Talebnia F, Aghaly Z, Mighari M (2015) Modelling of alkali pretreatment of rice husk using response surface methodology and artificial neural network. Chem Eng Commun 202(6):728–738
26. Prabh SM, Meenakshi S (2014) Enriched fluoride sorption using chitosan supported mixed metal oxides beads: synthesis, characterization and mechanism. J Water Process Eng 2:96–104
27. Ranasinghe J, Hansima MACK, Nanayakkara N (2022) Adsorptive removal of fluoride from water by chemically modified coal fly ash: Synthesis, Characterization, Kinetics and Mechanism. Ground water for sustainable Development 16(6):100699. doi: 10.1016/j.gsd.2021.100699
28. Rojas MCK, Bonilla PA, Sánchez RFJ, Moreno PJ, Reynel ÁHE, Aguayo VIA, Mendoza CDI (2015) Breakthrough curve modeling of liquid-phase adsorption of fluoride ions on aluminum-doped bone char using micro-columns: effectiveness of data fitting approaches. J Mol Liq 208:114–121
29. Saha D, Bhowal A, Datta S (2010) Artificial neural network modeling of fixed bed biosorption using radial basis approach. Heat Mass Transfer 46:431–436
30. Sahu N, Bhan C, Singh J (2020a) Removal of fluoride from an aqueous solution by batch and column process using activated carbon derived from iron infused *Pisum sativum* peel: characterization, isotherm, kinetics study. Environ Eng Res 26(4):1–11
31. Sahu RC, Patel RK, Ray BC (2010) Neutralization of red mud using CO_2 sequestration cycle. J Hazard Mater 179(1–3):28–34
32. Sivasankar V, Ramachandra MT, Chandramohan A (2010) Fluoride removal from water using activated and MnO_2 coated tamarind fruit (*Tamarindus indica*) shell: batch and column studies. J Hazard Mater 177:719–729
33. Tor A, Danaoglu N, Arslan G, Cengeloglu Y (2009) Removal of fluoride from water by using granular red mud: batch and column studies. J Hazard Mater 164:271–278
34. Wan K, Huang L, Yan J, Ma B, Huang X, Luo Z, Zhang H, Xiao T (2021) Removal of fluoride from industrial wastewater by using different adsorbent: A review. Sci Total Environ 773:145–535
35. Wang J, Chen N, Feng C, Li M (2018) Performance and mechanism of fluoride adsorption from groundwater by Lanthanum-modified pomelo peel bio char. Environ Sci Pollut Res Int 25(16):15326–15335
36. Wang XJ, Zhoo XY, Li QG, Chan TW, Wu SZ (2016) Artificial neural network modelling and mechanism study for relaxation of deformed rubber. Ind Eng Chem Res 55(14):4059–4070
37. Ye Y, Yang J, Jiang W, Kang J, Hu Y, Hao H (2018) Fluoride removal from water using a magnesia-pullulan composite in a continuous fixed-bed column. J Environ Manage 206:929–937
38. Yetilmezsoy K, Demirel S (2008) Artificial neural network (ANN) approach for modeling of Pb (II) adsorption from aqueous solution by Antep pistachio (*Pistacia vera* L.) shells. J Hazard Mater 153:1288–1300

39. Zare K, Banihashemi A, Jayanbakht V, Mohammadifard H (2022) Fluoride removal from aqueous solutions using alginate beads modified with functionalized silica particles. J Mol Struct 1252:132217. doi: 10.1016/j.molstruc.2021.132217

Tables

Table 1. Maximum removal measurements of F- from water using a fixed bed column technique on to various adsorbents.

Different adsorbents	Type of treatment	pH	F^- mg/g	References
Synthetic Al_2O_3/CeO_2 composite	Aqueous solution	6	9.72	Chen et al. 2021
Activated and MnO_2 coated tamarind fruit	Water	6.5	2.564	Sivasankar et al. 2010
Granular red mud	Water	4.7	1.274	Tor et al. 2009
Magnesia-pullulan composite	Water	7	16.6	Ye et al. 2018
rGO/ZrO_2 nanocomposite	Aqueous solution	7	45.7	Mohan et al. 2017.
Activated carbon derived from iron infused Pisum sativum peel	Aqueous solution	7	3.75	Sahu et al. 2020a
Lanthanum oxide–coated biochar	Water	6	24.75	Chakraborty and Das 2022
Graphene oxide–coated biochar	Water	6	11	Chakraborty and Das 2022
Zirconium Oxide-Coated Scoria	Water	6	0.058	Geleta et al. 2022
Neutralized activated red mud	Aqueous medium	7	3.815	Present study

Table 2 Analytical outcomes of fixed bed column parameters.

C_0 (Initial concentration, mg/L)	Bed height (cm), Z	Q_v (Flow rate $mLmin^{-1}$)	pH	M $_{adsorbent}$ (g)	V_B (mL)	t_B (min)	C_B (mg/g)	q_B (mg/g)
1	5	0.5	7	6.50	210	30	0.815	2.734
1	10	0.5	7	12	217	60	0.820	2.950
1	15	0.5	7	18.5	223	120	0.825	3.815

Table 3. Parameters predicted by Adams-Bohart and Thomas model at different fixed column bed height, at neutral pH, constant adsorbate concentration and flow rate of the solutions.

C_0 (Initial concentration, ppm)	Bed height (cm), Z	Q (Flow rate mL/min)	K_{AB} x 10^{-4} (L/mg min)	N_0 (mg/L)	R^2	RMSE
Adams-Bohart model						
1	5	0.5	8.44	124.67	0.948	0.211
1	10	0.5	18.94	118.34	0.904	0.111
1	15	0.5	23.62	113.58	0.901	0.120
C_0 (Initial concentration, ppm)	Bed height (cm), Z	Q (Flow rate mL/min)	K_{TH} x 10^{-4} (L/min mg)	q_0 (mg/g)	R^2	RMSE
Thomas model						
1	5	0.5	30.31	17.390	0.981	0.153
1	10	0.5	33.34	17.608	0.966	0.104
1	15	0.5	42.00	17.825	0.992	0.133

Table 4. Differentiation of experimental analysis results and predicted output results by ANN model of inference data set.

Exp. No.	Bed height (cm)	Initial concentration (mg/L)	Contact time (min)	Flow rate (mL/min)	Actual adsorption (%)	Predicted adsorption (%)	Residual (%)	(%) error	Absolute error (%)
1	15	1	10	0.5	85.11	84.9976	0.1124	0.132064	0.132064
2	15	1	15	0.5	85.07	84.7944	0.2756	0.323968	0.323968
3	15	1	20	0.5	89.24	88.3401	0.8999	1.0084	1.0084
4	15	1	25	2.5	88.24	89.1302	-0.8902	-1.0088	1.0088
5	10	1	30	2.5	83.21	84.4803	-1.2703	-1.52661	1.52661
6	10	1	35	2.5	87.04	87.0811	-0.0411	-0.04722	0.04722
7	10	5	40	2.5	86.21	86.0977	0.1123	0.13026	0.13026
8	10	5	45	2.5	80.05	80.489	-0.4391	-0.54841	0.5484
9	5	10	50	5.5	81.55	81.1587	0.3913	0.479828	0.479828
10	5	10	55	5.5	80.51	80.2694	0.2406	0.298844	0.298844
11	5	10	60	5.5	79.48	80.1682	-0.6882	-0.8658	0.8658
12	5	10	65	5.5	78.45	79.5125	-1.0625	-1.37227	1.37227
13	5	10	70	0.5	77.426	77.9345	-0.5085	-0.65676	0.65676
14	15	10	75	0.5	76.395	77.3455	-0.9505	-1.24491	1.24491
15	15	5	30	0.5	75.364	75.7895	-0.4255	-0.56459	0.564592
16	15	5	95	0.5	74.333	73.3659	0.9671	1.301037	1.301037
17	15	5	110	0.5	73.302	73.2625	0.0395	0.053887	0.053886
18	15	5	20	0.5	72.271	72.621	-0.35	-0.48429	0.484229
19	10	1	35	2.5	71.24	71.8066	-0.5666	-0.79534	0.795343
20	10	1	10	2.5	70.209	69.4716	0.7374	1.050292	1.050292
21	10	1	15	5.5	67.178	70.3689	-1.1909	-1.7215	1.72152
22	10	1	25	5.5	84.21	84.9976	-0.7876	-0.93528	0.93528
23	10	10	135	5.5	87.44	86.7944	0.6456	0.738334	0.738334
24	10	10	140	0.5	85.11	86.3401	-1.2301	-1.44531	1.44531
25	5	10	45	0.5	81.05	81.1302	-0.0802	-0.09895	0.09895
26	5	10	55	0.5	82.35	82.4803	-0.1303	-0.15823	0.158227
27	5	10	60	2.5	82.419	81.0811	1.3379	1.62329	1.62329
28	5	10	10	2.5	80.488	80.0977	0.3903	0.484912	0.484912
29	5	10	15	2.5	81.457	81.489	-0.032	-0.03928	0.039284
30	15	1	20	2.5	79.426	79.1587	0.2673	0.336539	0.336539
31	15	5	25	2.5	82.395	82.2694	0.1256	0.152436	0.152436

32	15	5	30	5.5	74.164	74.1682	-0.00042	-0.00057	0.00057
33	15	5	35	5.5	75.333	76.5125	-1.1795	-1.56571	1.56571
34	15	5	40	5.5	73.402	73.9345	-0.5352	0.725457	0.725457
35	15	5	45	5.5	73.271	73.3455	-0.0745	-0.10168	0.101677
36	5	5	50	0.5	74.24	74.7895	-0.5495	-0.74017	0.74017
37	5	1	55	0.5	66.209	70.3659	-1.1569	-1.6716	1.67161
38	5	1	60	0.5	70.178	70.2625	-0.0845	-0.12041	0.12041
39	5	5	65	0.5	73.41	73.621	-0.211	-0.28748	0.28748
40	15	5	70	0.5	72.86	72.8066	0.0534	0.073291	0.073291
41	15	5	75	0.5	69.209	70.3659	-1.1569	-1.6716	1.67161
42	15	1	30	2.5	70.178	70.2625	-0.0845	-0.12041	0.12041

Figures

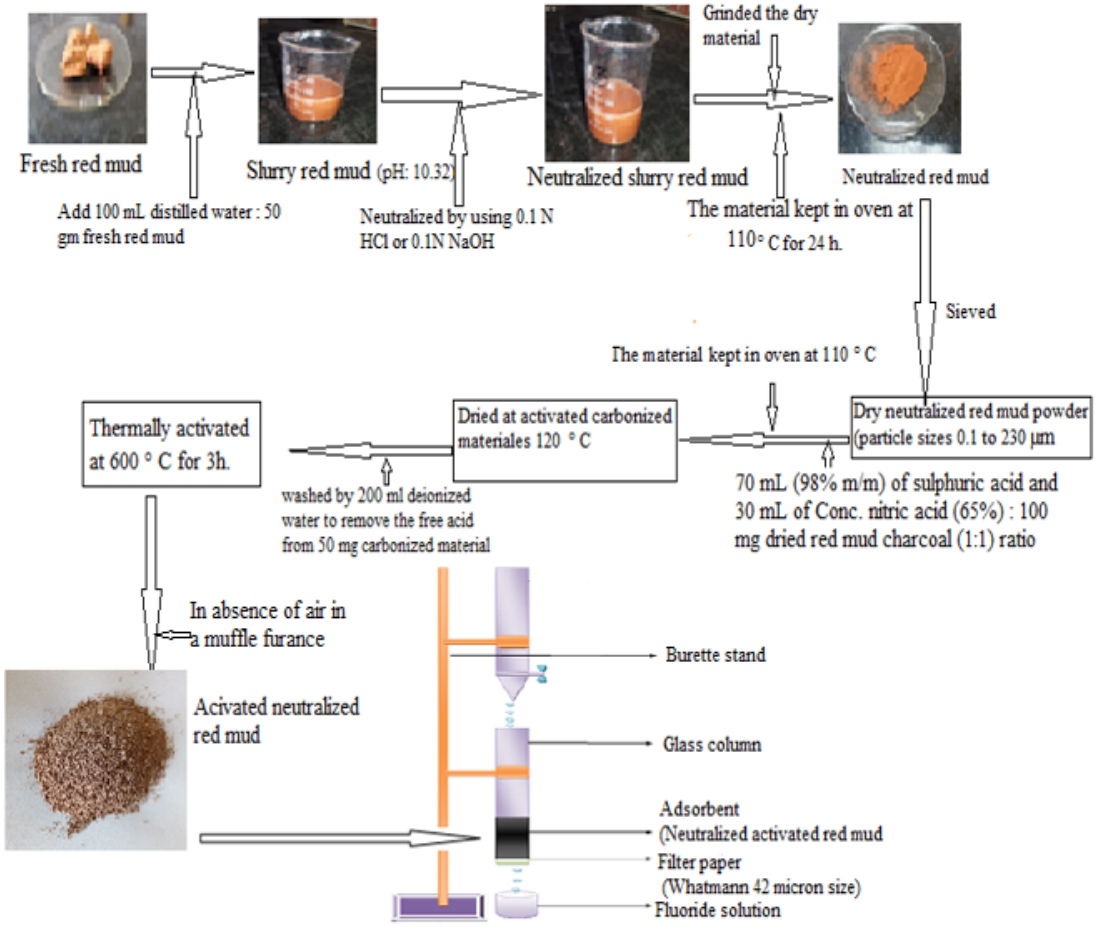

Figure 1

Devising approach flow chart of neutralized activated red mud derived from fresh red mud.

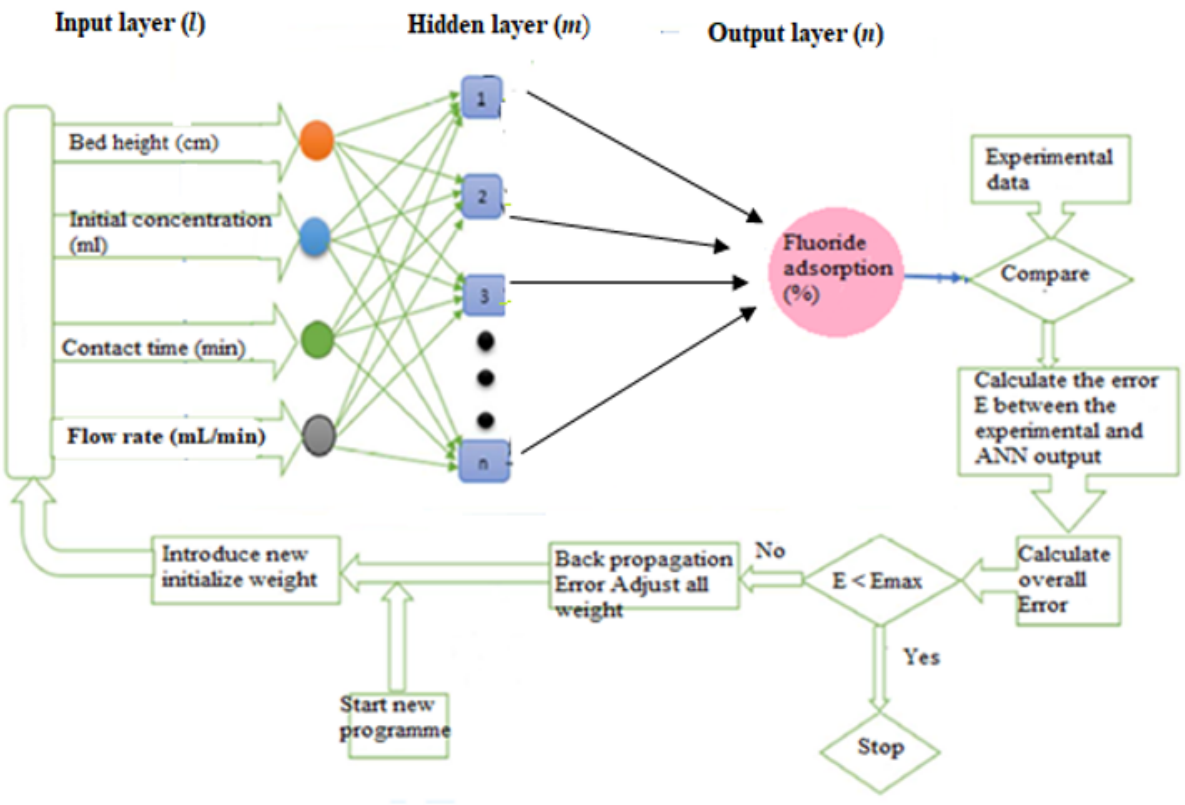

Figure 2

Optimum ANN model with a flowchart of the backpropagation algorithm for the prediction of F^- removal efficiency.

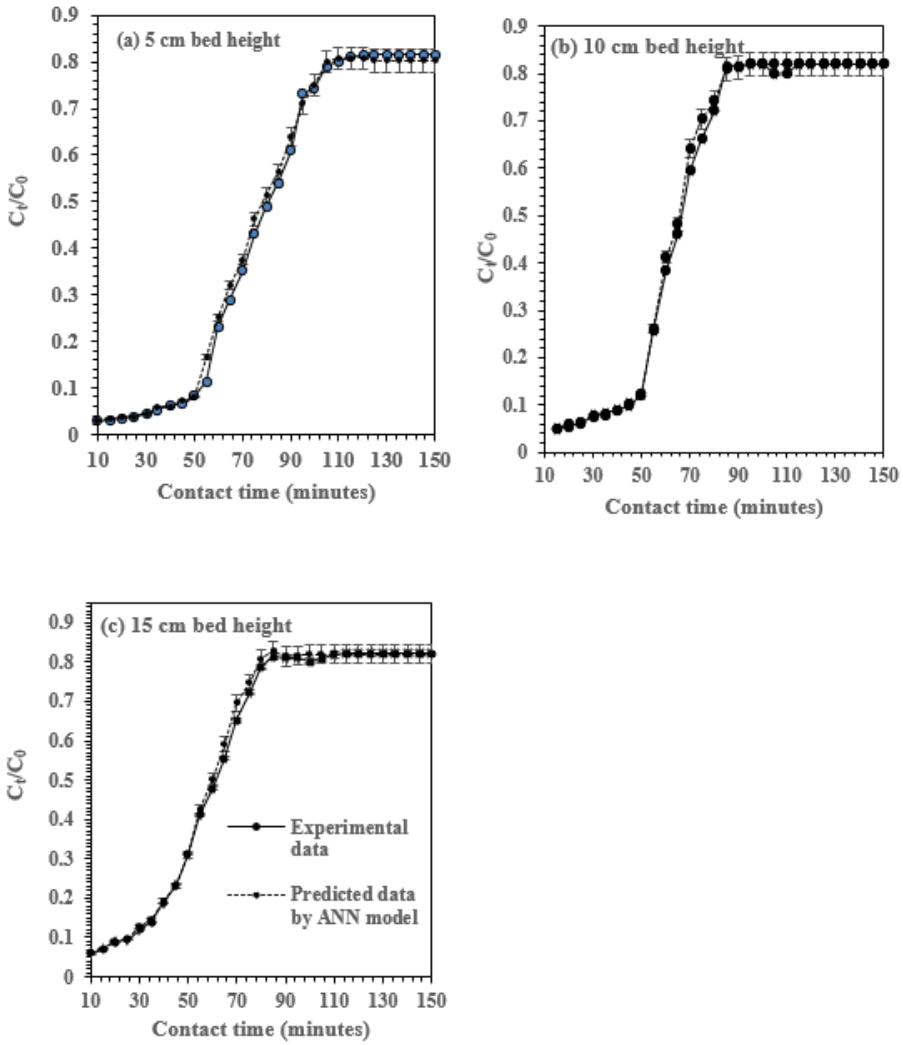

Figure 3

Experimental data and predicted results by ANN as a consequence of (a) 5 cm, (b) 10 cm and (c) 15 cm bed heights with experimental time on the removal of F- in a continuous fixed bed column. (Initial concentration: 1 mg/L; flow rate: 0.5 mL/min; pH:7; and temperature: 30 ± 2 ◻ C).

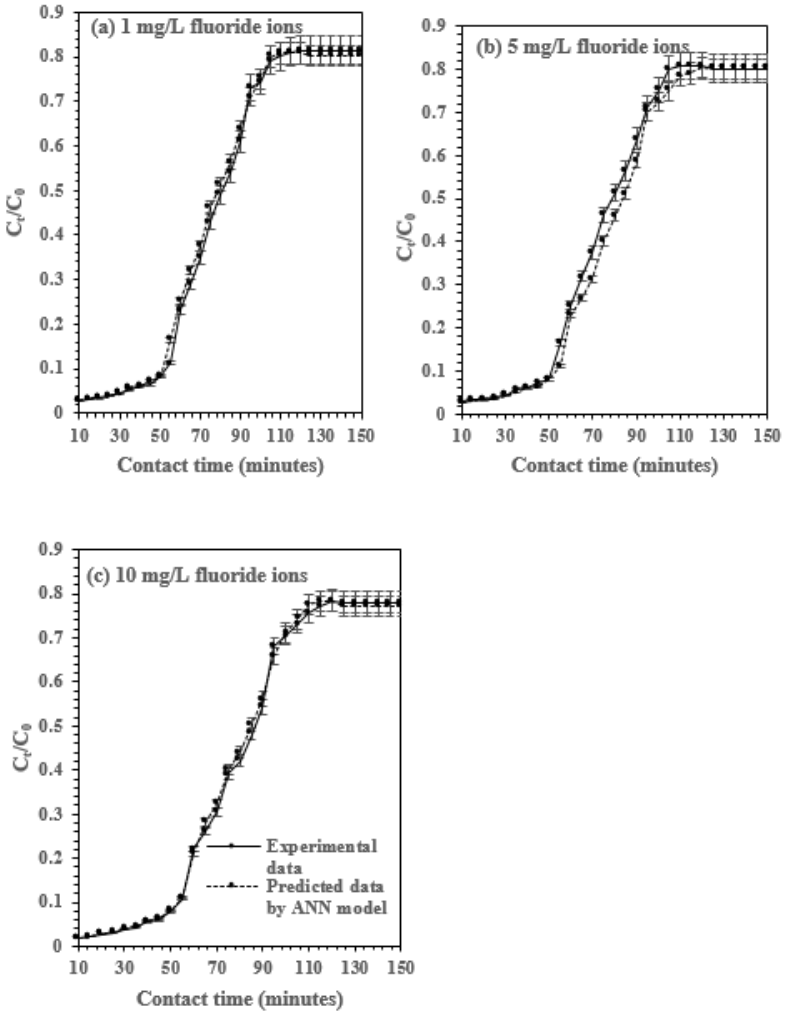

Figure 4

Experimental data and predicted results by ANN as a consequence of (a) 1 ppm, (b) 5 ppm, and (c) 10 ppm F- concentrations with experimental time on the removal of F- in a continuous fixed bed column. (Bed height: 15cm; flow rate: 0.5 mL/min; pH:7; and temperature: 30 ± 2 □ C).

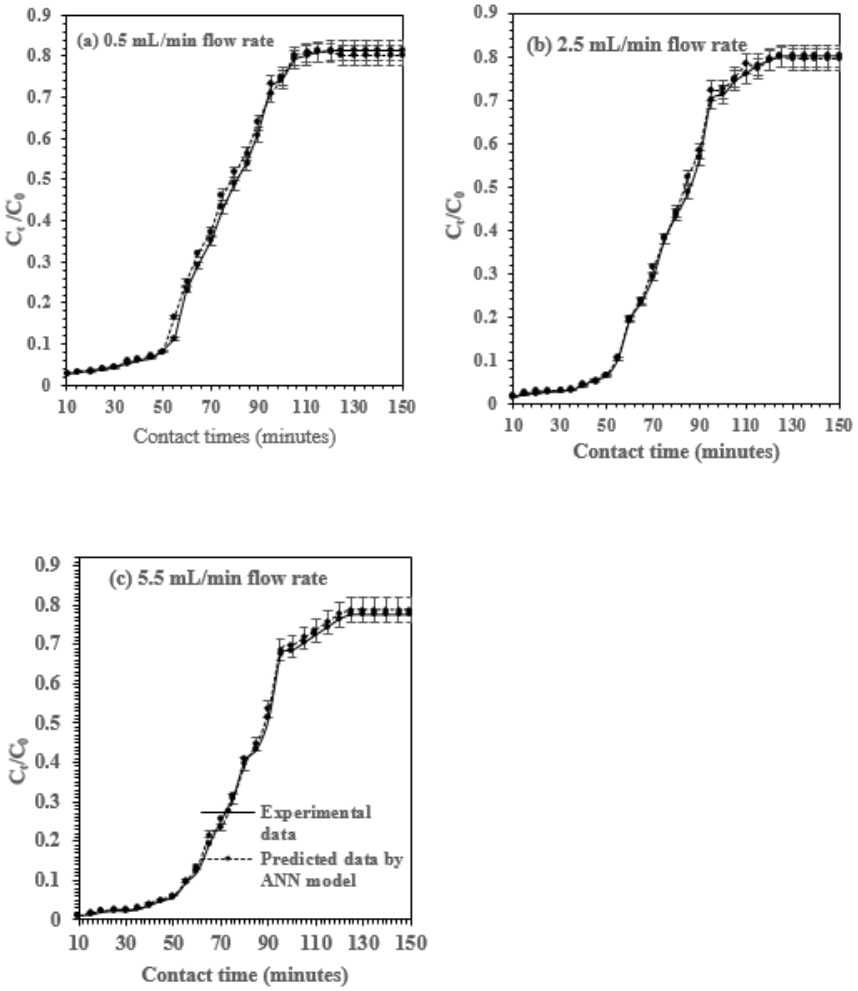

Figure 5

Experimental data and predicted results by ANN as a consequence of (a) 0.5 mL/min, (b) 2.5 mL/min, and (c) 5.5 mL/min flow rate with experimental time on the removal of F- in a continuous fixed bed column. (Initial concentration: 1 mg/L; bed height:15 cm; pH:7; and temperature: 30 ± 2 ◻ C).

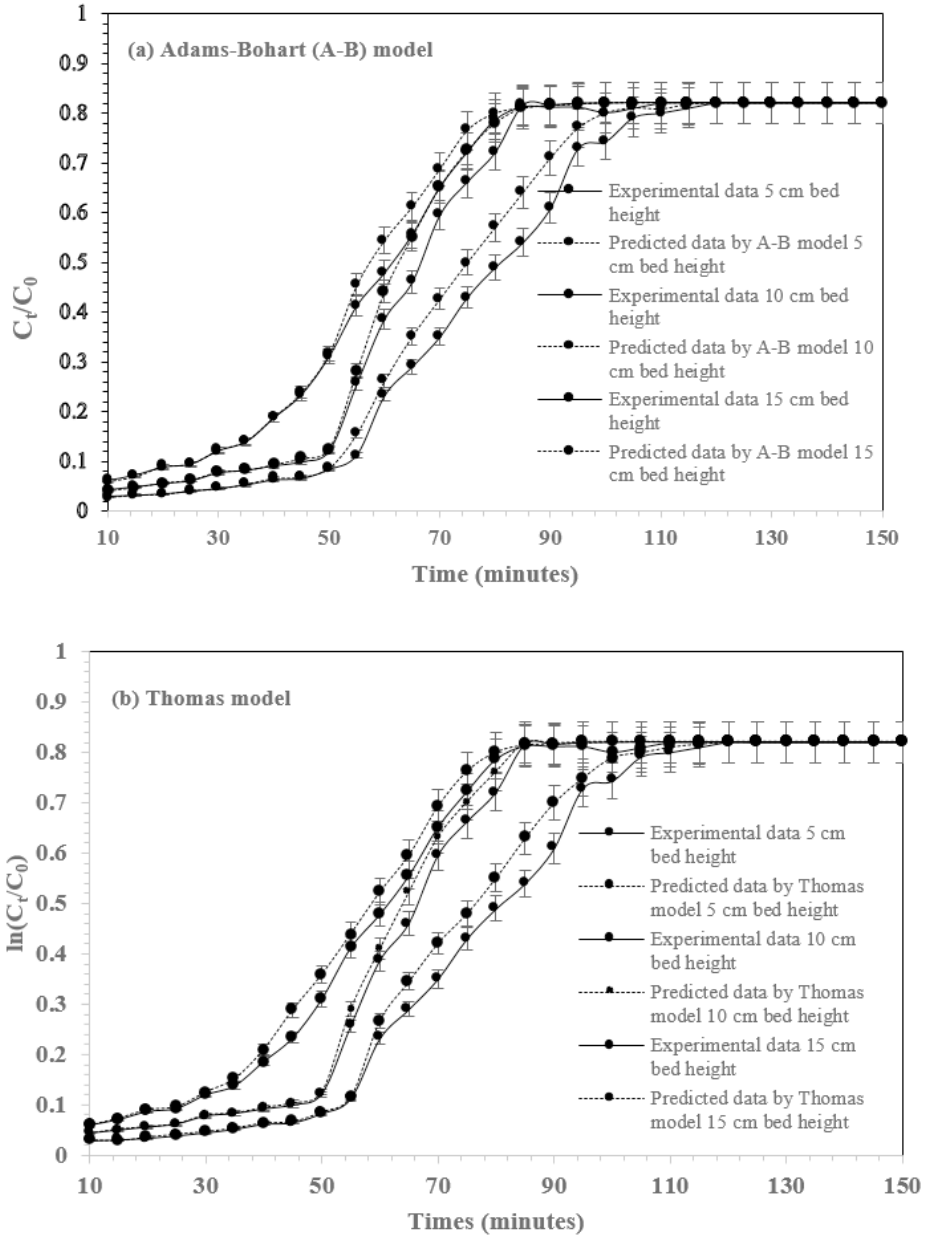

Figure 6

Consequence of fixed bed column bed height on F- removal predicted by (a) Adams-Bohart model, and (b) Thomas model.

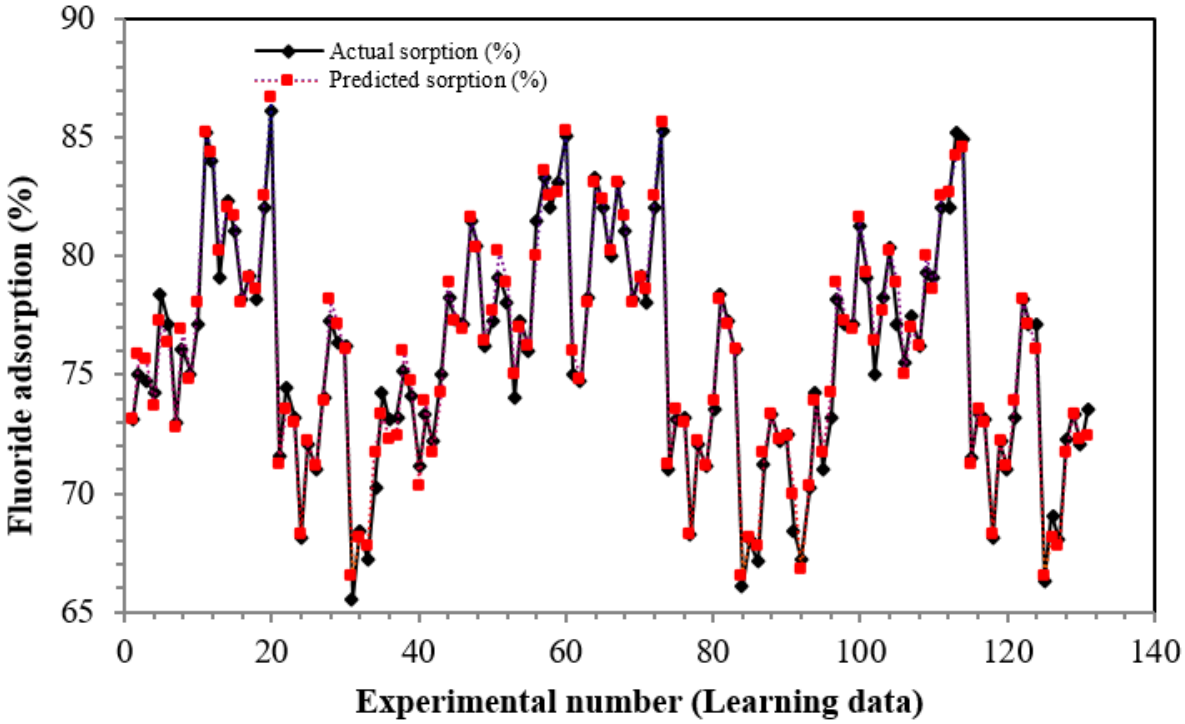

Figure 7

Dissemination of fluoride removal percentage of learning data set.

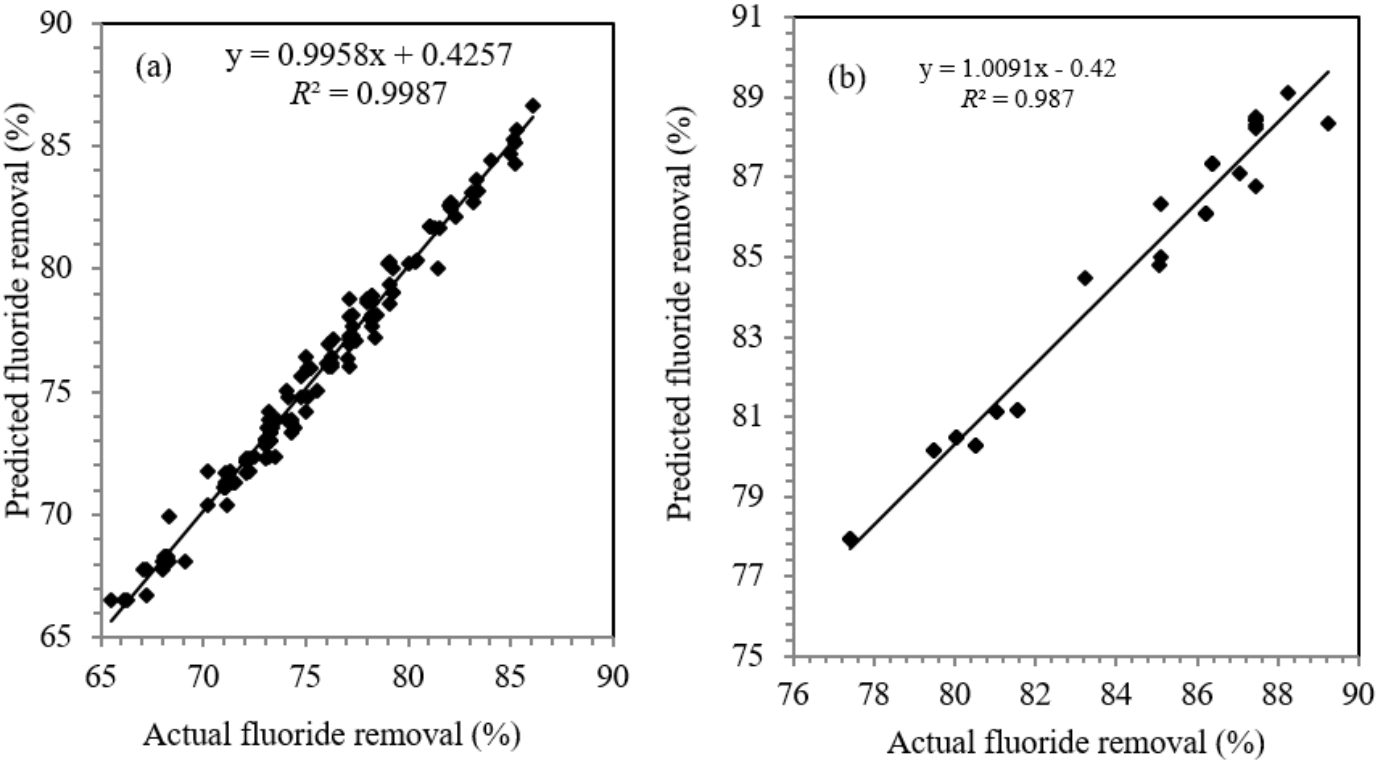

Figure 8

(a) Correlation of predicted and actual F- removal percentage of (a) Learning data set and (b) Inference data set.

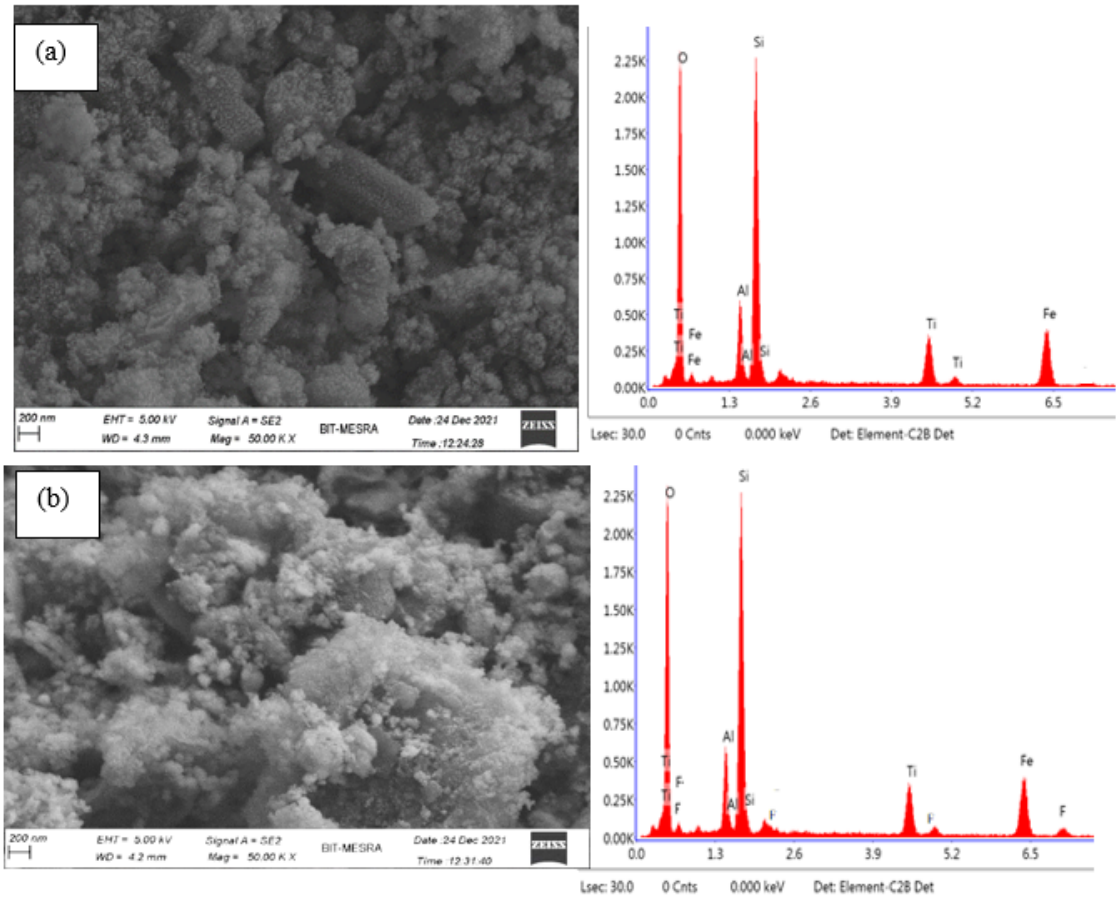

Figure 9

SEM-EDS analysis of (a) before and (b) after treatment of F- 1ppm using NARM.

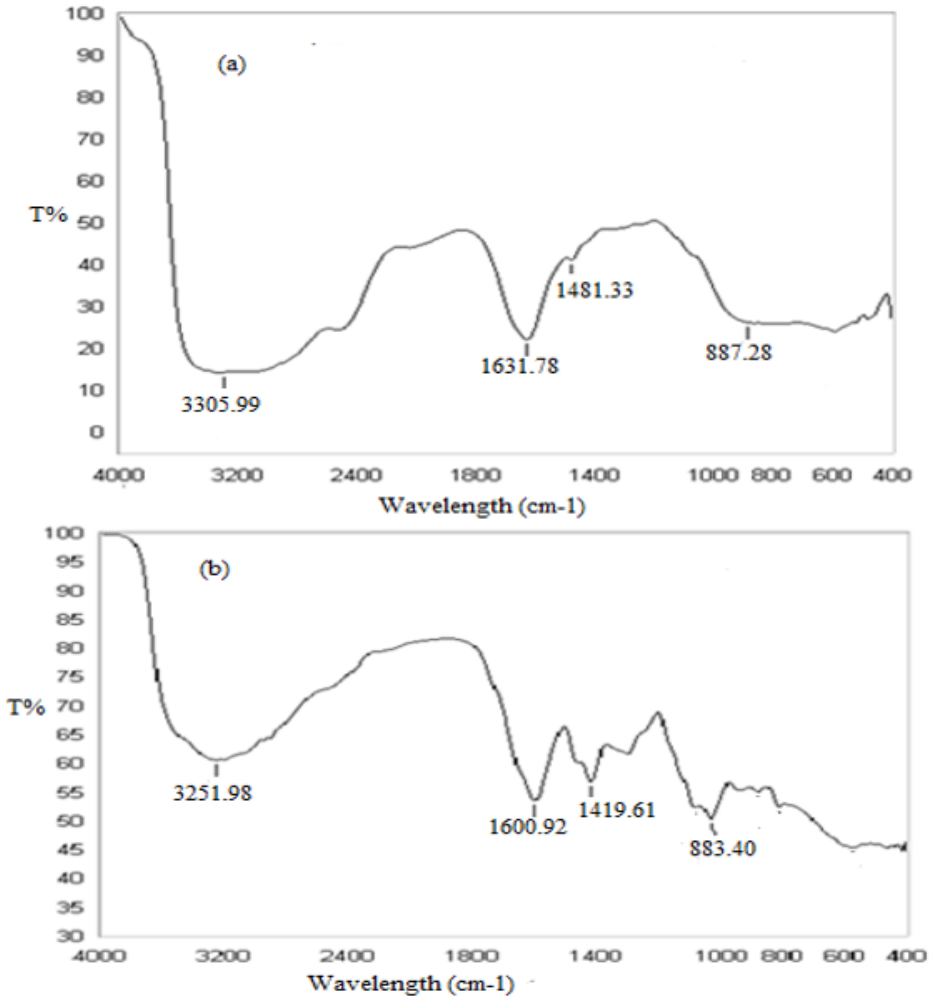

Figure 10

FTIR analysis of (a) control and (b) loaded F- 1 ppm.

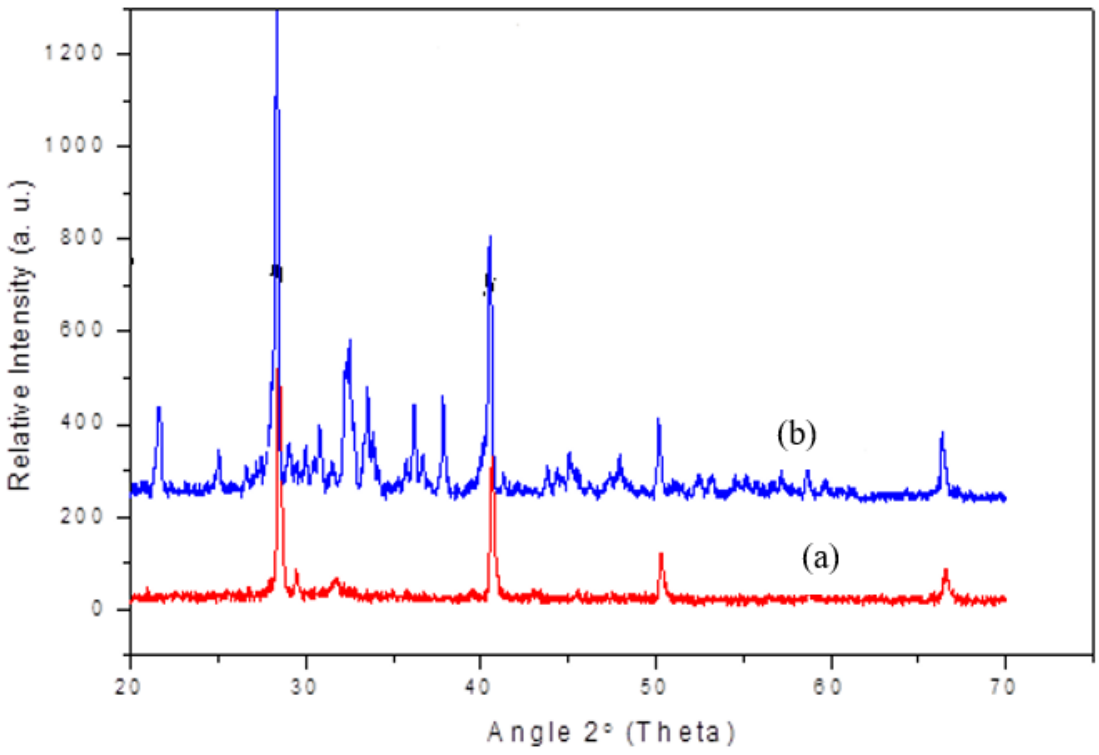

Figure 11

X-ray diffraction pattern of NARM, (a) Before adsorption, (b) after adsorption of F-.

Supplementary Files

This is a list of supplementary files associated with this preprint. Click to download.

- Suplementarymaterial.docx